processes

Article

Spray Cooling Schemes and Temperature Field Analysis of Ultra-High-Temperature Production Wells in Underground Coal Gasification

Yang Tang [1,2,*], Haoyu Xiong [1,2], Yin He [1,2], Shunxiao Huang [1,2] and Yuan Wang [1,2]

[1] School of Mechatronic Engineering, Southwest Petroleum University, Chengdu 610500, China; xhy13678056375@163.com (H.X.); heyin_ww@163.com (Y.H.); sydoncrazy@126.com (S.H.); wangyuan980521@163.com (Y.W.)
[2] Energy Equipment Institute, Southwest Petroleum University, Chengdu 610500, China
* Correspondence: tangyanggreat@swpu.edu.cn

Abstract: In underground coal gasification (UCG), it is essential for UCG production to accurately control the temperature of the gas produced at the wellhead of the production well and correctly calculate the variation law of the temperature field in the whole wellbore. UCG wellbore structures use three wellbore sprayed water cooling schemes. These schemes consider the heat exchange mechanism between the wellbore and the formation, the division of the production wellbore into the spray chamber section and the non-spray section, and the established temperature field model of the whole wellbore. The research shows that, due to the large temperature gradient formed in the wellbore heat transfer route under the spray tubing water injection cooling scheme, the temperature of the produced gas drops the most. The annular water injection cooling scheme can protect the cement sheath to a certain extent and is easier to implement; therefore, it is more suitable to use this scheme to cool the production well. It is feasible to control the temperature of the production wellhead by controlling the temperature of the spray chamber. The greater the daily output of produced gas or the thermal conductivity of the tubing, the smaller the temperature change between the bottom hole and the wellhead, and the more the spray water temperature rises.

Keywords: underground coal gasification; wellbore heat transfer; spray cooling; temperature field; gasifier

check for updates

Citation: Tang, Y.; Xiong, H.; He, Y.; Huang, S.; Wang, Y. Spray Cooling Schemes and Temperature Field Analysis of Ultra-High-Temperature Production Wells in Underground Coal Gasification. *Processes* **2022**, *10*, 1149. https://doi.org/10.3390/pr10061149

Academic Editor: Blaž Likozar

Received: 25 May 2022
Accepted: 6 June 2022
Published: 8 June 2022

1. Introduction

Traditional coal mining methods have low utilization efficiency, have a great impact on the environment [1], and accidents often occur during the mining process. As a new chemical coal mining technology, UCG is the process of controlling the combustion of underground coal seams and generating combustible gas through chemical and thermal effects [2–4]. During UCG, the temperature of the underground gasification chamber can be as high as 1200 °C [5,6], and high-temperature crude gas is produced on the surface through a production well. After reaching a steady state, the wellhead temperature of the production well is about 600 °C. If the wellhead is not cooled down by spraying water, the high temperature will cause risks such as wellhead uplift and casing deformation, which will seriously affect the gas well's production life and wellbore integrity [7,8]. In the spraying process, it is necessary to adjust the amount of sprayed water in the production wellbore according to different production conditions to ensure the wellhead temperature and the temperature requirements of the produced gas. However, different spraying schemes will have a more significant impact on the cooling effect of the wellhead device, structural design, and production process. Therefore, a reasonable spraying scheme plays a vital role in the production cost and operational safety of UCG.

There has been much analysis of the wellbore temperature field. Ramey considered the thermal resistance of the wellbore and assumed that the heat conduction in the wellbore is steady, and the heat conduction to the surface is unsteady [9]. Alves considered the influence of the Joule–Thomson effect on the energy equation and the influence of well inclination, single-phase flow, and two-phase flow and established a comprehensive wellbore transient temperature model [10]. Hasan regarded the wellbore as a heat sink with a finite radius in an infinitely active medium, considered the heat transfer resistance of various components of the wellbore, established a robust model of two-phase flow in a geothermal well by using the drift flux method, simulated the heat transfer between wellbore fluid and formation, and compared it with other models [11]. Mao established the wellbore transient temperature field model during horizontal well drilling, discretized the model with the finite volume method, and solved it with the underrelaxation iterative method [12]. Gao analyzed the dissociation of hydrate by establishing a heat transfer model between the deep water drilling of wellbores and reservoirs, combined with the physical and physical equilibrium of hydrate [13]. Cheng presented a new formation heat-transfer model considering wellbore heat capacity and obtained a novel analytical transient heat transfer time function that depends on dimensionless time and the ratio of formation heat capacity and wellbore heat capacity [14]. Wang calculated the temperature distribution of heavy oil wells based on the coupling of an electromagnetic field and a temperature field. In order to improve the accuracy of temperature calculation, temperature-dependent reservoir thermos-physical parameters were specifically considered in the heat transfer equation and wave equation [15]. Li proposed a coupled reservoir/wellbore model of horizontal wells in a steam injection, which considers the three-dimensional simultaneous flow of three phases in the reservoir and the gas–liquid two-phase flow in the wellbore [16]. Xiao considered both the heat source and variations in the thermophysical properties of drilling fluids and tubular string with temperature and pressure, established a transient heat transfer model for high-temperature wells during the drilling process, and used an iterative method to calculate the annular temperature distributions [17]. Mao presented a wellbore transient model that depends on the boundary conditions at a finite radial distance from the wellbore [18]. You proposed a fully implicit numerical model of wellbore heat transfer, in which the fluid energy equation is treated as transient; however, the wellbore part still adopts Ramey's steady-state heat transfer assumption [19]. Song improved on the Ramey model, only considering the wellbore fluid as a steady state, changed the wellbore medium to unsteady heat transfer, and analyzed the temperature field distribution of the wellbore gas production process [20]. Zhong established a time and space of unsteady pressure drop and heat transfer differential equation system based on the conservation of mass, momentum and energy during the blowout test process, and used the Newton–Raphson method to solve the equations [21].

At present, research on the high-temperature wellbore temperature field mainly includes steam huff and puff high temperature for heavy oil thermal recovery, electric heating heavy oil thermal high temperature, and other wellbore types [22–24]. However, the maximum temperature of these wellbores does not exceed 300 °C. In addition, none of these studies analyzed the temperature field of a high-temperature wellbore under the spray cooling state. In order to ensure the safety of UCG, it is necessary to analyze the production well temperature in the state of ultra-high-temperature spray cooling and reasonably control its temperature.

Because of the temperature characteristics of UCG production wells, firstly, we propose three different spray cooling schemes and establish temperature field models of the wellbore during the spray cooling process. Secondly, a more suitable spraying scheme is discussed based on the cooling effect of the produced gas and engineering difficulty. Finally, the sensitivity of wellbore temperature field parameters is analyzed, which plays a guiding role in wellbore spray cooling and wellbore design in UCG.

2. Heat Transfer Model

2.1. Model Assumptions

The spray cooling of the production well can be achieved in three ways: spray tubing water injection cooling, annulus water injection cooling and concentric tubing water injection cooling. A heat transfer model is established for each working condition, and differential equations are solved. Since heat transfer is involved during casing, cement sheath, and formation spraying, and in order to simplify the calculation, the following assumptions need to be made before establishing the wellbore temperature field prediction model:

(1) All parameters in the same section in the wellbore are consistent, and the gas in the wellbore flows stably in one dimension.

(2) From the wellbore to the second interface (the interface between the cement sheath and the formation) and then to the formation, there is one-dimensional stable heat transfer and one-dimensional unstable heat transfer.

(3) Ignoring the heat transfer along the well depth, and the radius of the heat loss in the wellbore and formation.

(4) The geothermal gradient is known, and the formation temperature along the radial direction varies linearly with depth and is axisymmetric, being distributed axially along the wellbore.

(5) The interfaces of casing, cement sheath and the formation of the surrounding rock are closely connected.

2.2. Spray Tubing Water Injection

Figure 1 shows the spray tubing water injection spray cooling of a UCG production well. A hanging spray tubing is positioned in the production tubing, nitrogen is injected into the annulus between the production tubing and technical casing, and the spray tubing is injected with sprayed water. The produced gas flows from the annulus between the production tubing and the spray tubing. The sprayed water exchanges heat with the produced gas during the water injection process.

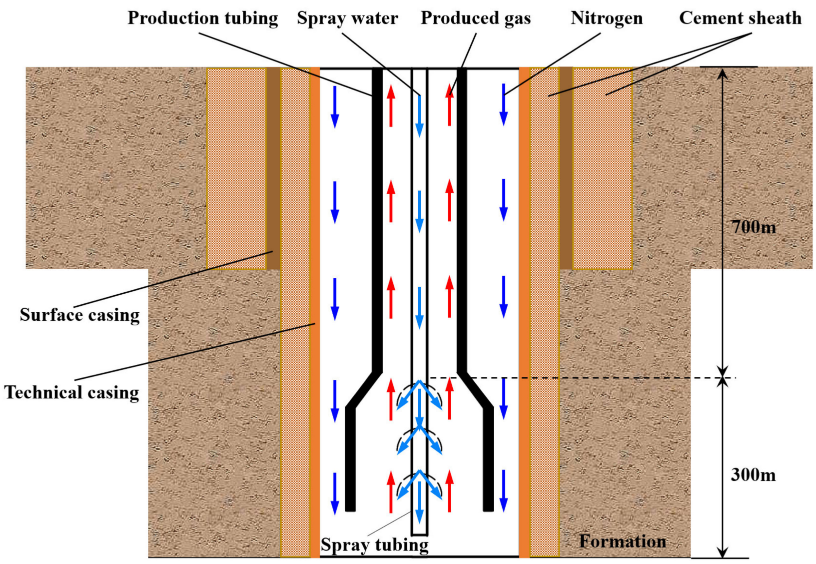

Figure 1. Spray tubing water injection spray cooling process.

Figure 2 shows a micro element of a wellbore cement sheath formation using spray tubing water injection. According to the principle of energy conservation, for a wellbore under steady heat transfer, the fluid temperature in the wellbore can be expressed as follows.

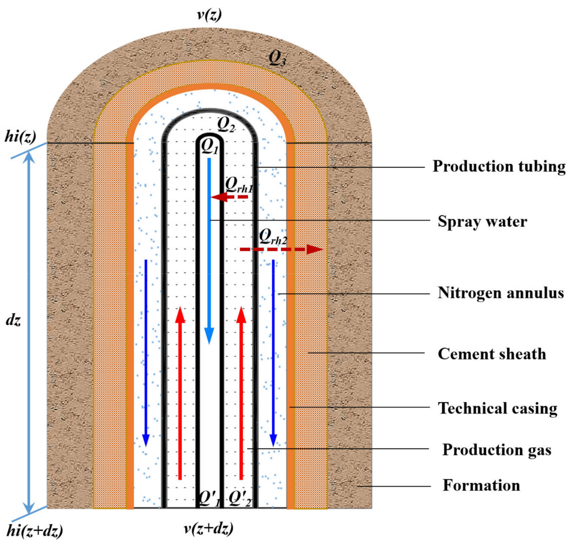

Figure 2. Calculation model of temperature field using spray tubing water injection cooling.

The energy conservation equation for spray is:

$$w_1 c_{p1} \frac{dT_1}{dz} + 2\pi r_d U_d (T_1 - T_2) = 0 \tag{1}$$

Moreover, the energy conservation equation of produced gas can be written as:

$$w_2 c_{p2} \frac{dT_2}{dz} - 2\pi r_d U_d (T_2 - T_1) - 2\pi r_h U_{h1} (T_2 - T_h) = 0 \tag{2}$$

The heat transferred from produced gas in the wellbore to the second interface is equal to the heat transferred from the second interface to the formation, and the expression can be described as:

$$Q = 2\pi r_h (T_2 - T_h) = \frac{2\pi k_c (T_h - T_e)}{f(t_D)} \tag{3}$$

The right side of Equation (3) represents the amount of heat transferred from the second interface to the formation. The heat diffusion of the wellbore fluid causes the temperature of the surrounding formation to gradually increase. Even under the condition of stable production, the heat diffusion from the wellbore to the formation will change with time, but as time increases, its rate of change becomes smaller, so we introduce a transient heat transfer function $f(t_D)$ to represent [25–27].

$$\begin{cases} f(t) = \lg\left(\frac{2(\alpha t_D)^{0.5}}{r_h/12}\right) - 0.29 & t_D > 1.5 \\ f(t) = 1.1281 {t_D}^{0.5} (1 - 0.3 {t_D}^{0.5}) & t_D < 1.5 \end{cases} \tag{4}$$

Combined with the above formulas, the general formula for calculating the wellbore temperature field when using spray tubing is obtained as follows:

$$w_2 c_{p2} \frac{dT_2}{dz} - 2\pi r_d U_d (T_2 - T_1) - \frac{2\pi r_h U_{h1} k_e (T_2 - T_e)}{r_h U_h f(t_D) + k_e} = 0 \tag{5}$$

Finally, by solving the differential Equations (1) and (5), the wellbore temperature field distribution of the spray tubing cooling method can be obtained.

Similarly, the expression of the cement sheath temperature field is:

$$T_c = \frac{f(t_D) r_h T_2 + k_e T_e}{k_e + f(t_D) r_h} \tag{6}$$

Under the condition of steady-state heat transfer, the total heat transfer parameters of the wellbore (tubing–casing–cement sheath) is:

$$U_{h1} = \left[\frac{r_{to}}{r_{ti}h_f} + \frac{r_{to}\ln\frac{r_{to}}{r_{ti}}}{k_{tub}} + \frac{r_{to}}{r_{co}\cdot(h_c+h_r)} + \frac{r_{to}\ln\frac{r_{to}}{r_{ci}}}{k_{cas}} + \frac{r_{to}\ln\frac{r_h}{r_{co}}}{k_e} \right]^{-1} \tag{7}$$

2.3. Annulus Water Injection

Figure 3 shows the annulus water injection spray scheme. In this scheme, spray water is injected from the annulus between the technical casing and the production tubing. The produced gas and the spray water exchange heat through the production tubing and then the heat is exchanged with the formation through the cement sheath and the surface casing.

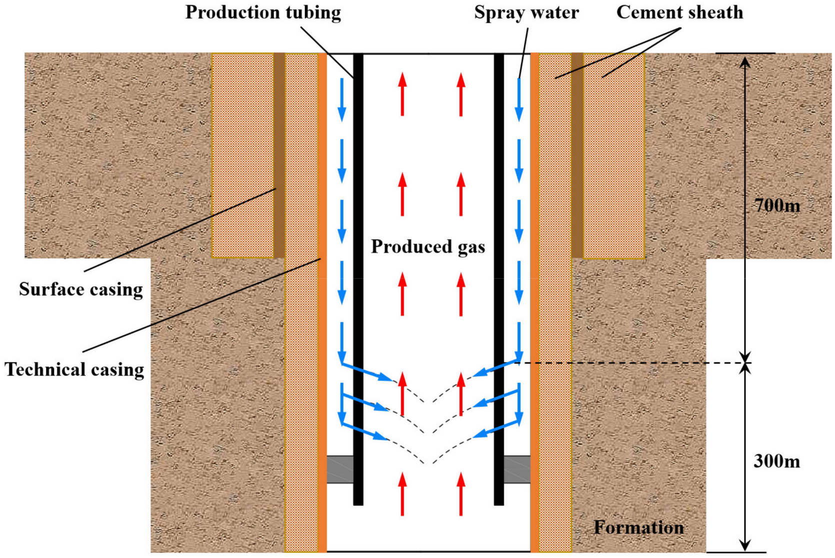

Figure 3. Annulus water injection spray cooling process.

Figure 4 shows a micro element of wellbore cement sheath formation under annulus water injection. The fluid temperature in the wellbore under annulus spray is expressed as follows:

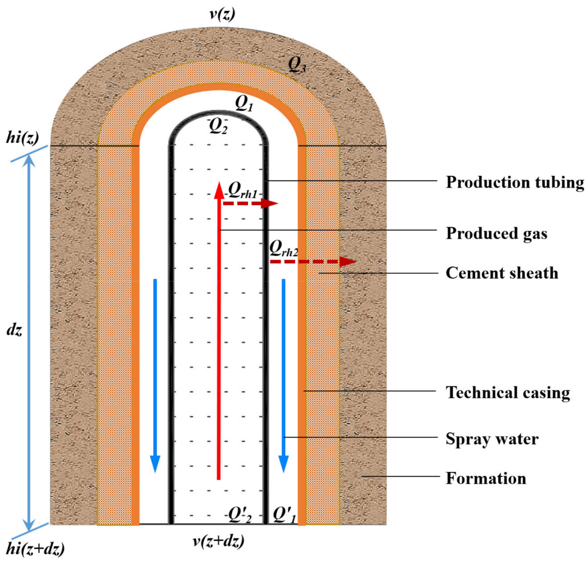

Figure 4. Temperature field calculation model of annular water injection spray.

The energy conservation equation of sprayed water is:

$$w_1 c_{p1} \frac{dT_1}{dz} - 2\pi r_{ti} U_t (T_1 - T_2) = 0 \quad (8)$$

The energy conservation equation of produced gas can be described as:

$$w_2 c_{p2} \frac{dT_2}{dz} + 2\pi r_{ti} U_t (T_1 - T_2) - 2\pi r_h U_{h2} (T_2 - T_h) = 0 \quad (9)$$

Moreover, the general calculation formula of a wellbore temperature field is expressed as follows:

$$w_2 c_{p2} \frac{dT_2}{dz} + 2\pi r_d U_d (T_1 - T_2) - \frac{2\pi r_h U_{h2} k_e (T_2 - T_e)}{r_h U_{h2} f(t_D) + k_e} = 0 \quad (10)$$

The temperature field expression of the cement sheath is:

$$T_c = \frac{f(t_D) r_h T_2 + k_e T_e}{k_e + f(t_D) r_h} \quad (11)$$

Under the condition of steady-state heat transfer, the total heat transfer parameters of a wellbore (casing–cement sheath) is:

$$U_{h2} = \left[\frac{r_{ti} \ln \frac{r_{co}}{r_{ci}}}{k_{cas}} + \frac{r_{ti} \ln \frac{r_h}{r_{co}}}{k_e} \right]^{-1} \quad (12)$$

2.4. Concentric Tubing Water Injection

Figure 5 is the UCG production well concentric tubing water injection scheme. In this scheme, concentric tubing is added between the production tubing and the technical casing, and the sprayed water is injected between the production casing and the concentric tubing. Nitrogen is injected into the annulus between the concentric tubing and the technical casing for heat insulation. Similarly, during the injection process, the sprayed water exchanges heat with the produced gas through the production tubing and the heat is then exchanged with the formation through the nitrogen annulus and the cement sheath.

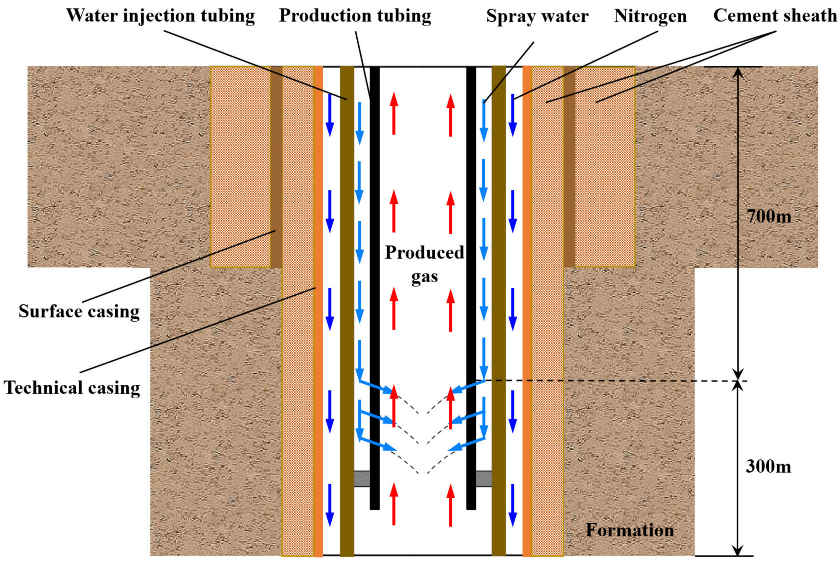

Figure 5. Concentric tubing water injection spray cooling process.

Figure 6 shows a micro element of a wellbore cement sheath formation using concentric tubing water injection. According to the calculation model of the temperature field of annular water injection, the calculation differential equations of the production wellbore temperature field using concentric tubing water injection spray cooling are similarly deduced as follows:

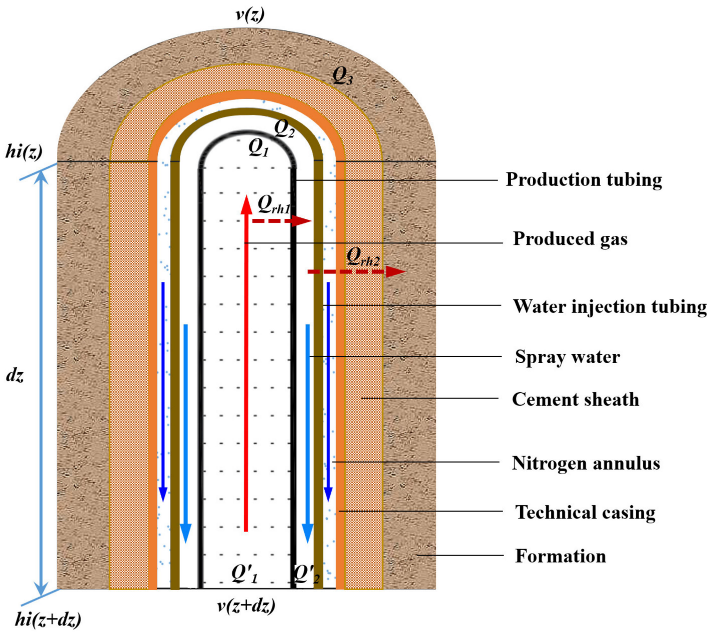

Figure 6. Calculation model of water injection spray temperature field in concentric tubing.

The energy conservation equation of sprayed water can be described as:

$$w_1 c_{p1} \frac{dT_1}{dz} - 2\pi r_{ti} U_t (T_1 - T_2) = 0 \tag{13}$$

The energy conservation equation of produced gas can be expressed as follows:

$$w_2 c_{p2} \frac{dT_2}{dz} + 2\pi r_{ti} U_t (T_1 - T_2) - 2\pi r_h U_{h3} (T_2 - T_h) = 0 \tag{14}$$

The general calculation formula of a wellbore temperature field is:

$$w_2 c_{p2} \frac{dT_2}{dz} + 2\pi r_d U_d (T_1 - T_2) - \frac{2\pi r_h U_{h3} k_e (T_2 - T_e)}{r_h U_{h3} f(t_D) + k_e} = 0 \tag{15}$$

The temperature field expression of the cement sheath is:

$$T_c = \frac{f(t_D) r_h T_2 + k_e T_e}{k_e + f(t_D) r_h} \tag{16}$$

The total heat transfer parameters of a wellbore (casing–annulus–cement sheath) under steady-state heat transfer can be written as:

$$U_{h3} = \left[\frac{r_{ti}}{r_{ti} h_f} + \frac{r_{ti}}{r_{co} \cdot (h_c + h_r)} + \frac{r_{ti} \ln \frac{r_{co}}{r_{ci}}}{k_{cas}} + \frac{r_{ti} \ln \frac{r_h}{r_{co}}}{k_e} \right]^{-1} \tag{17}$$

3. Temperature Field Analysis of a Spray Wellbore

3.1. Analysis of Spray Water Consumption

For the convenience of calculation, the wellbore is divided into a spray chamber section and a non-spray section.

Assuming that the spray water in the spray chamber is completely gasified and the spray target temperature is reached at the top of the spray chamber, the heat absorbed by the spray water is equal to the heat released by the produced gas, that is, the relationship between the spray amount, output and the target temperature is as follows:

$$Q_g\rho\left(C_{Pl2}\times T_{p2}-C_{Pl2}{}'\times T_{p2}{}'\right)=\mathrm{G}\left(C_{Pl1}{}'\times T_{p1}{}'-C_{Pl1}\times T_{p1}\right) \tag{18}$$

By setting the spray water temperature at the outlet to 50 °C and analyzing the amount of spray water at different gas outputs and different target temperatures, as shown in Figure 7, when the target temperature is constant, the higher the gas production, the greater the spray amount.

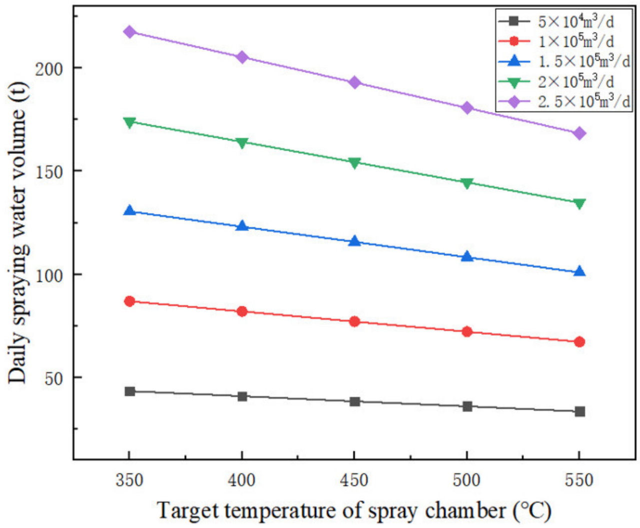

Figure 7. Relationship between spray water volume and target temperature under different levels of gas production.

3.2. Analysis of Temperature Field in Spray Wellbore

Before solving the model, it is necessary to define boundary conditions and initial conditions.

Boundary conditions are as follows:

The temperature of the spray water injected into the production wellhead T_2 is known and constant,

$$T_2 = T_{in} = const \tag{19}$$

The formation temperature is a known function of depth,

$$T_e = T_e(h) \tag{20}$$

The external boundary condition is defined as the temperature at the wireless distance from the wellbore equal to constant geological temperature,

$$T_e(r=\infty) = const \tag{21}$$

The inner boundary condition is defined as the interface between the cement sheath and the formation,

$$T_e(r=r_h) = T_h \tag{22}$$

Initial conditions are as follows:

The wellbore temperature is reduced to 400 °C at a depth of 700–1000 m.

The spray water temperature at the wellhead is set at 30 °C.

The temperature field calculation models of the three spray cooling processes were respectively calculated, and the temperature field relationship between the spray water and the produced gas was obtained. Table 1 shows the relevant parameters.

Table 1. Parameters of wellbore structure and working conditions.

Category	Value
Well depth, m	1000
Outer diameter of casing, mm	177.8
Inner diameter of casing, mm	160
Outer diameter of tubing, mm	114
Inner diameter of tubing, mm	100
Borehole size, mm	445
Target temperature of spray chamber, °C	400
Daily output of produced gas, m^3/d	2×10^5
Spray water consumption, t/d	350
Thermal conductivity of insulation tubing, W/(m·°C)	2.5
Thermal conductivity of tubing and casing, W/(m·°C)	100
Thermal conductivity of cement sheath, W/(m·°C)	2.5
Specific heat capacity of produced gas, W/(m·°C)	3200

3.2.1. Analysis of Wellbore Temperature Field in Spray Tubing Water Injection

As shown in Figure 8, the temperature of spray water increases slowly from the wellhead to the bottom of the well, reaching about 50 °C at a depth of 700 m, while the temperature of produced gas decreases by about 200 °C from the bottom of well to the wellhead, and the temperature at the wellhead is about 205 °C; however, the temperature of the cement sheath slowly decreases from 95 °C at the bottom of well to 75 °C at the wellhead.

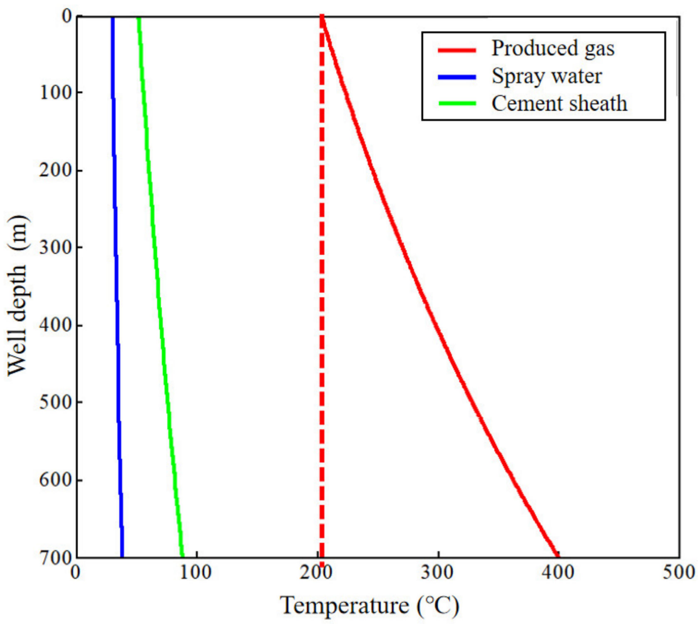

Figure 8. Temperature distribution of spray tubing injection wellbore.

3.2.2. Analysis of Temperature Field using Water Injection in a Wellbore Annulus

Figure 9 shows that the temperature of spray water changes little from the wellhead to the bottom of well. The temperature of the produced gas drops by about 150 °C from the bottom of the well to the wellhead, and the produced gas temperature at the wellhead is about 250 °C. In contrast, the temperature of cement sheath remains basically unchanged because the heat from the underground gas is absorbed by the spray water. The cement sheath temperature is slightly higher than the spray water temperature because the formation temperature increases with the increase in the well depth.

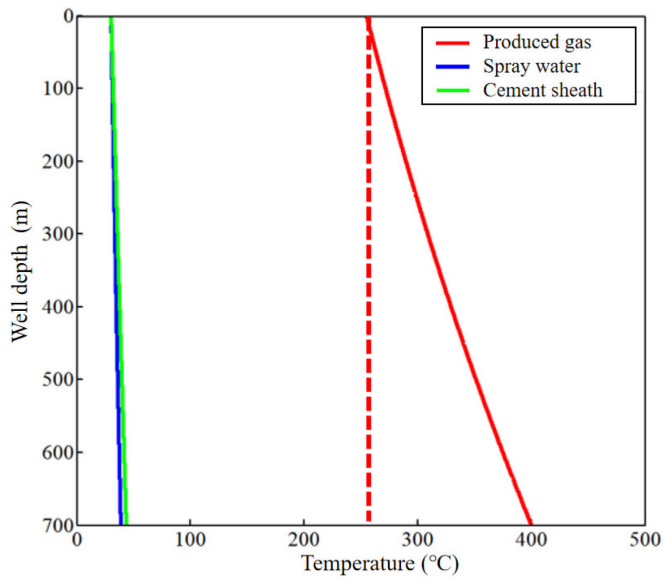

Figure 9. Temperature distribution of annulus water injection wellbore.

3.2.3. Analysis of Temperature Field in Annular Water Injection in Concentric Tubing

As can be seen from Figure 10, the temperature of spray water increases slightly from the wellhead to the bottom of the well. In contrast, the produced gas temperature decreases by about 140 °C from the bottom of the well to the wellhead, and the wellhead gas temperature is about 250 °C. There is little difference between the wellbore temperature curve under the annulus spray cooling condition. Although the nitrogen annulus is added, the cooling effect is not obvious.

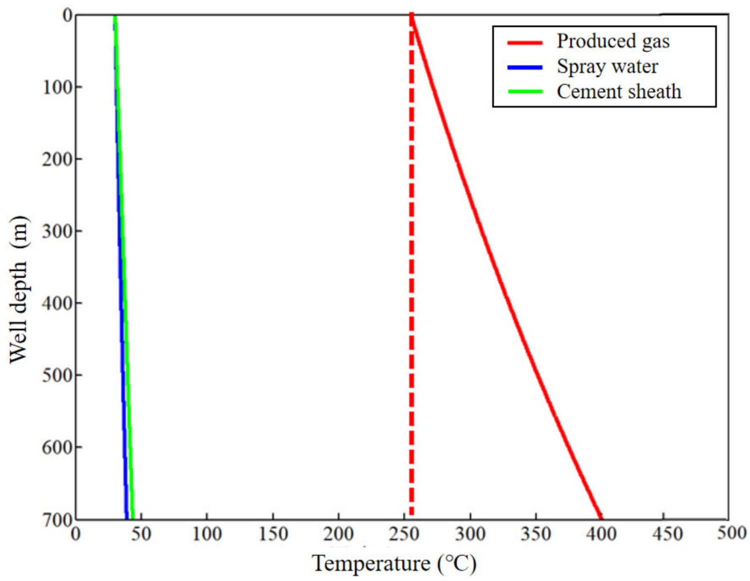

Figure 10. Temperature distribution of concentric water injection wellbore.

3.3. Spray Scheme Selection

From the above analysis, it can be found that the temperature of the produced gas decreases the most by using the spray tubing spray cooling scheme because the heat from the produced gas needs to be transferred to the water in the spray tubing and the formation at the same time, forming two different high temperature heat transfer processes. However, the annulus water injection and concentric tubing water injection are a single produced gas–spray water–formation heat transfer process. The temperature gradient formed in their heat transfer route is small, so the heat transfer is less than that of the spray tubing scheme.

The overall temperature field distribution of a 0–1000 m wellbore can be obtained by combining the cooling of the spray chamber and the cooling of the wellbore. It can be seen from Figure 11 that spray cooling decreases the temperature the most at a well depth of between 700 m and 1000 m, followed by the wellbore 0–700 m section, because the water in the spray chamber is directly gasified and absorbs heat. Although the cooling effect of the produced gas is better under the spraying method of the spray pipe, in terms of process selection, the cement sheath in the non-spraying section can be better protected by the annular water injection cooling method. It is also simpler and more feasible than the spray tubing and concentric tubing water injection schemes.

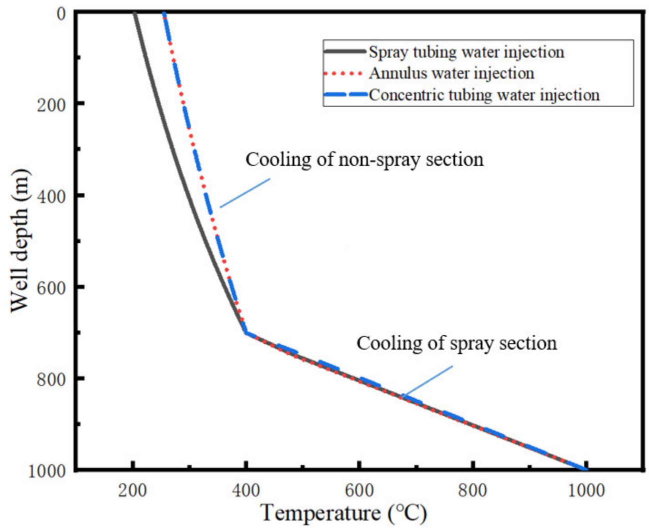

Figure 11. Distribution of produced gas temperature field after wellbore spraying.

4. Sensitivity Analysis of Wellbore Temperature Field Parameters after Spraying

The previous description analyzed the distributions of the wellbore temperature field under three spraying schemes, and the annulus water injection spraying process was selected. However, in the spraying process, the amount of spray water, the daily output of produced gas, and the thermal conductivity parameters of tubing are also closely related to the temperature field after spraying, which is of great significance when considering the spray amount.

4.1. Daily Output of Produced Gas

It can be seen below that when the daily output of produced gas is 5×10^4–2.5×10^5 m^3/d, spray water is under different spray target temperatures. Analysis of the temperature field distribution of produced gas in the wellbore range of non-spray section under the same target temperature of the spray chamber and different daily output is shown in Figure 12. The temperature decreases by about 100 °C at 2.5×10^5 m^3/d and 300 °C at 5×10^4 m^3/d, which indicates that the greater the gas output production, the smaller the impact of spray cooling on the variation in the wellbore temperature field within the well depth range, and this trend becomes more and more evident with the increase in gas production. Because the output changes from 2.5×10^5 m^3/d to 2×10^5 m^3/d, the difference in the produced gas temperature is significantly less than 1×10^5 m^3/d to 5×10^4 m^3/d. When the daily output is 5×10^4 m^3/d, the temperature of the spray water increases by about 33 °C due to a lesser spray amount, as shown in Figure 13, while in the case of high output, the temperature of produced gas does not change much, and the higher the output, the more stable it is.

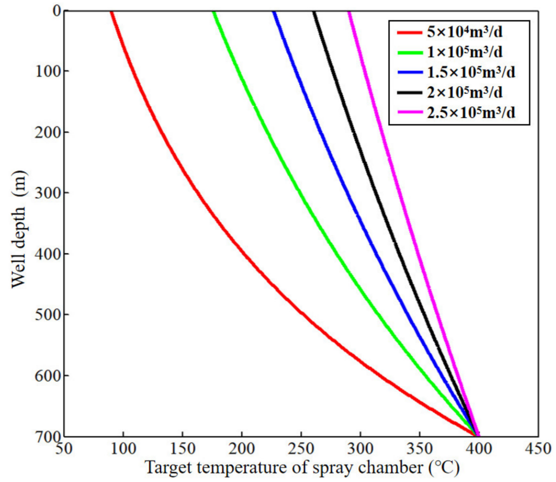

Figure 12. Temperature distribution of produced gas under different outputs.

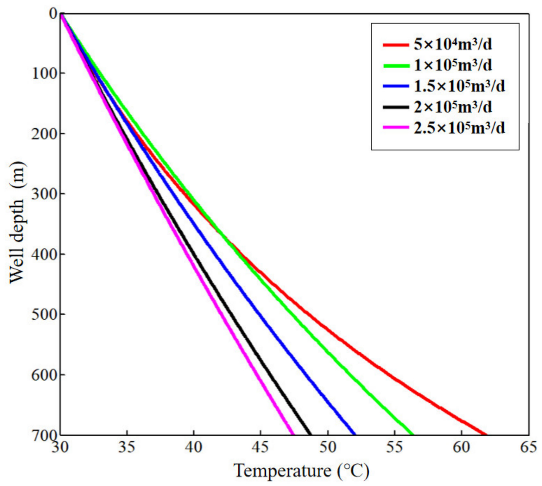

Figure 13. Temperature distribution of spray water under different outputs.

4.2. Target Temperature of Spray Chamber

As shown in Figure 14, when the spray chamber temperature is set to be 350–550 °C, there is little difference in the decreased range of produced gas temperature, which shows that it is feasible to control the wellhead temperature by controlling the spray chamber temperature.

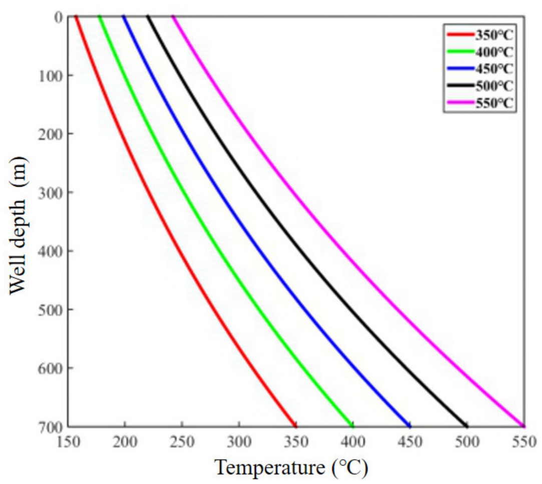

Figure 14. Temperature distribution of produced gas at different spray chamber temperatures.

4.3. Thermal Conductivity of Production Tubing

Different thermal conductivities have apparent effects on the temperature of spray water and produced gas. The temperature field conditions of production tubing thermal conductivity of 2.5–12.5 W/m·°C were analyzed with gas production, spray water amount, and other conditions. As shown in Figures 15 and 16, as the thermal conductivity of the tubing increases, the more the produced gas temperature decreases and the more the spray water temperature increases. Because the production tubing is located between the spray water and the produced gas, it directly determines the heat exchange efficiency between them, which is significant for the temperature control of the spray water and produced gas.

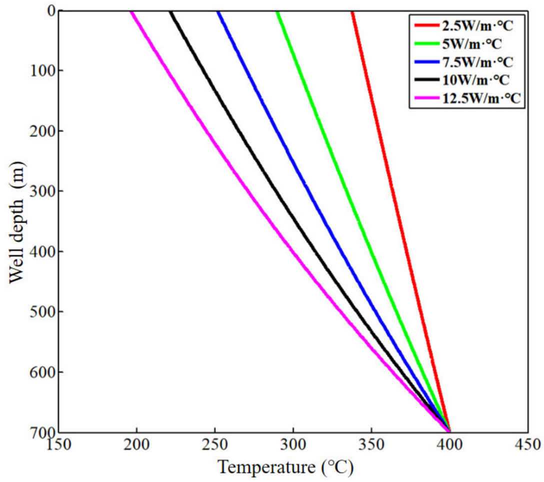

Figure 15. Temperature distribution of produced gas using different thermal conductivities of production tubing.

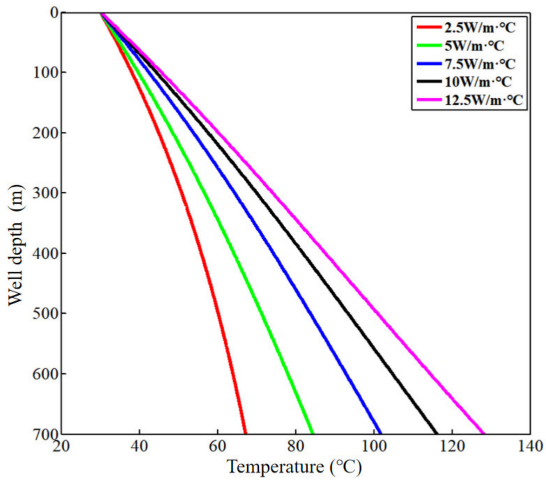

Figure 16. Temperature distribution of spray water using different thermal conductivities of production tubing.

4.4. Total Thermal Conductivity of Cement Sheath Casing

Under certain other conditions, analyzing the wellbore temperature distribution is important when the total thermal conductivity is 6–14 W/m·°C. It can be seen from Figures 17 and 18 that different total thermal conductivity parameters have little effect on the temperature distribution of spray water in the wellbore. The greater the total thermal conductivity, the smaller the increase in spray water temperature. This is because after the increase in total thermal conductivity, the heat transfer from produced gas to formation increases, so the temperature difference between produced gas and spray water decreases, and the heat transferred becomes less. However, under the different total thermal conductivity, the temperature of the produced gas hardly changes, which shows that the total thermal conductivity of the cement casing has little effect on the wellbore temperature distribution after spraying.

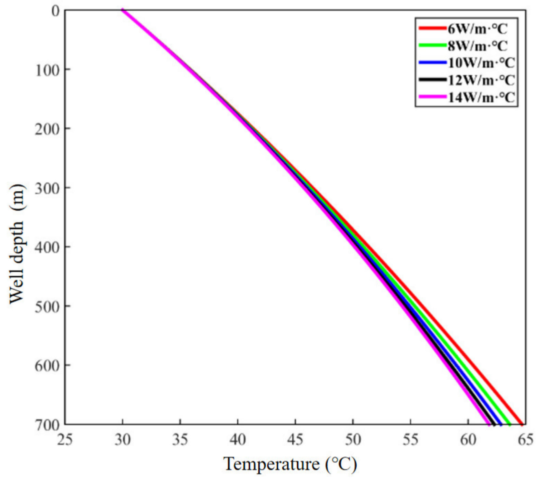

Figure 17. Temperature distribution of spray water using different total heat transfer coefficients of cement sheath casing.

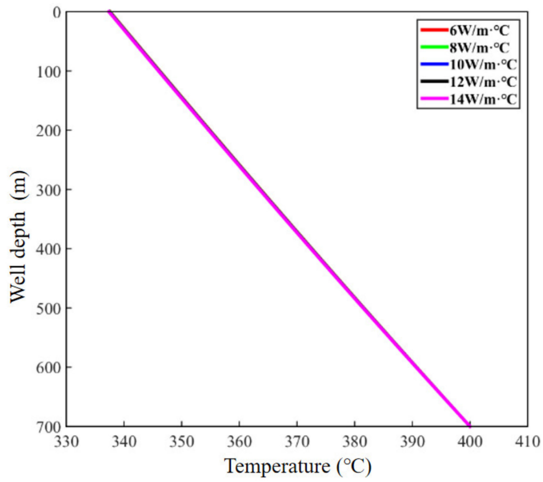

Figure 18. Temperature distribution of produced gas using different total heat transfer coefficients of cement sheath casing.

5. Conclusions

In this paper, we studied the temperature fields of production wellbores in the process of UCG. Based on the principle of energy conservation and the heat transfer law, three schemes of the wellbore temperature field using spray cooling were analyzed, and the conclusions are as follows:

(1). Using the same target temperature for the spray chamber, the spray tubing water injection spray cooling scheme has a better cooling effect. The annulus water injection spray cooling scheme can protect the cement sheath at the bottom of well and is easier to implement. Considering this, the annulus water injection spray method is preferable.

(2). With the increase in gas production, the temperature from the bottom of well to wellhead increases, and this trend becomes more obvious with the increase in production. In the process of UCG, excessive gas production will easily lead to excessive high wellhead temperatures of the production well and increase production risk.

(3). Using different temperatures in the spray chamber, the variation trend of the produced gas temperature changes in a similar way, which indicates that the wellhead temperature can be controlled indirectly by controlling the temperature of the spray chamber.

(4). The thermal conductivity of production tubing has a great influence on the temperature change in the produced gas. With the increase in the thermal conductivity of production tubing, the temperature of the produced gas decreases more, while the total thermal conductivity of the cement sheath casing has little effect on the temperature of the produced gas.

Author Contributions: Conceptualization, methodology, writing—original draft: Y.T., Y.H. and H.X. Writing—editing and reviewing: H.X., S.H. and Y.W. Supervision, investigation: H.X. All authors have read and agreed to the published version of the manuscript.

Funding: This work was funded by the National Natural Science Foundation of China (grant numbers 52004235), China; the National Key Research and Development Program (grant numbers 2021YFC2800903), China; China Postdoctoral Science Foundation (grant numbers 2020M683359), China; International Science and Technology Cooperation Project Funding (grant numbers 2020-GH02-00041-HZ), China; National Science and Technology Major Project (grant numbers 2016ZX05028-001-006), China; China Postdoctoral Innovative Talents Support Program (grant numbers BX20190292), China; and Sichuan Province Applied Basic Research Project (grant numbers 2020YJ0152), China.

Conflicts of Interest: The authors declare no conflict of interest.

Nomenclature

C_{p1}	Specific heat capacity of spray water, KJ/(kg·°C);
C_{pl1}	Specific heat capacity of spray water at T_{p1}, KJ/(kg·°C);
$C_{pl1'}$	Specific heat capacity of steam at $T_{p1'}$, KJ/(kg·°C);
C_{p2}	Specific heat capacity of produced gas, KJ/(kg·°C);
C_{pl2}	Specific heat capacity of produced gas at T_{p2}, KJ/(kg·°C);
$C_{pl2'}$	Specific heat capacity of produced gas at $T_{p2'}$, KJ/(kg·°C);
G	Spray water volume, t/d;
T_e	Formation temperature, °C;
T_h	Second interface temperature (interface between cement sheath and stratum), °C;
T_1	Spray water temperature, °C;
T_2	Produced gas temperature, °C;
T_c	Cement sheath temperature, °C;
T_{p1}	Water temperature before spraying, °C;
$T_{p1'}$	Water vapor temperature after spray water gasification, °C;
T_{p2}	Initial temperature of produced gas, °C;
$T_{p2'}$	Temperature of produced gas after spraying, °C;
Q_g	Daily output of produced gas, m^3/d.
r_{ci}	Casing inner diameter, m;
r_{co}	Casing outer diameter, m;
r_d	Outer diameter of spray pipe, m;
r_h	Outer diameter of cement sheath, m;
r_{ti}	Tubing inner diameter, m;
r_{to}	Tubing outer diameter, m;
U_d	Thermal conductivity of spray pipe, W/(m·°C);
U_{h1}	Total heat transfer coefficient of wellbore (tubing-casing-cement sheath), W/(m^2·°C);
U_{h2}	Total heat transfer coefficient of wellbore (casing-cement sheath), W/(m^2·°C);
U_{h3}	Total heat transfer coefficient of wellbore (casing-annulus-cement sheath), W/(m^2·°C);
U_t	Thermal conductivity of tubing, W/(m·°C);
k_{cas}	Thermal conductivity of casing, W/(m·°C);
k_c	Thermal conductivity of cement sheath, W/(m·°C);
k_{tub}	Thermal conductivity of tubing, W/(m·°C);
k_{gas}	Thermal conductivity of produced gas, W/(m·°C);
$f(t_D)$	Formation transient heat transfer function;
t_D	Heat transfer time, h;
h_c	Annular convective heat transfer coefficient, W/(m·°C);
h_f	Film heat transfer coefficient, W/(m·°C);

h_r Annular radiation heat transfer coefficient, W/(m·°C);
ρ ·Density of produced gas, kg/m^3;
w_1 Spray water volume, t/d;
w_2 Produced gas production, t/d.

References

1. Bhutto, A.W.; Bazmi, A.A.; Zahedi, G. Underground coal gasification: From fundamentals to applications. *J. Prog. Energy Combust. Sci.* **2013**, *39*, 189–214. [CrossRef]
2. Yang, L.H.; Liang, J.; Yu, L. Clean coal technology-Study on the pilot project experiment of underground coal gasification. *J. Energy* **2003**, *28*, 1445–1460. [CrossRef]
3. Khan, M.M.; Mmbaga1, J.P.; Shirazi, A.S.; Trivedi, J.; Liu, Q.X.; Gupta, R. Modelling Underground Coal Gasification—A Review. *J. Energies* **2015**, *8*, 12603–12668. [CrossRef]
4. Yang, L.H. Study on the model experiment and numerical simulation for underground coal gasification. *J. Fuel* **2004**, *83*, 573–584. [CrossRef]
5. Shahbazi, M.; Najafi, M.; Marji, M.F. On the mitigating environmental aspects of a vertical well in underground coal gasification method. *J. Mitig. Adapt. Strateg. Glob. Chang.* **2019**, *24*, 373–398. [CrossRef]
6. Seifi, M.; Chen, Z.X.; Abedi, J. Numerical Simulation of Underground Coal gasification Using the Crip Method. *J. Can. J. Chem. Eng.* **2011**, *89*, 1528–1535. [CrossRef]
7. Zheng, S.J.; Li, W.; Cao, C.G.; Wang, C. Prediction of the wellhead uplift caused by HT–HP oil and gas production in deep-water wells. *J. Energy Rep.* **2021**, *7*, 740–749. [CrossRef]
8. Zheng, S.G.; Zhang, C.Z. Influence of Cement Return Height on the Wellhead Uplift in Deep-Water High-Pressure−High-Temperature Wells. *J. ACS Omega* **2021**, *6*, 2990–2998. [CrossRef]
9. Ramey, H.J. Wellbore Heat Transmission. *J. Pet. Technol.* **1962**, *14*, 427–435. [CrossRef]
10. Alves, I.N.; Alhanati, F.J.S.; Shoham, O. A Unified Model for Predicting Flowing Temperature Distribution in Wellbores and Pipelines. *J. SPE Prod. Eng.* **1992**, *7*, 363–367. [CrossRef]
11. Hasan, A.R.; Kabirb, C.S. Modeling two-phase fluid and heat flows in geothermal well. *J. Pet. Sci. Eng.* **2010**, *71*, 77–86. [CrossRef]
12. Mao, L.J.; Zhang, Z. Transient temperature prediction model of horizontal wells during drilling shale gas and geothermal energy. *J. Pet. Sci. Eng.* **2018**, *169*, 610–622. [CrossRef]
13. Gao, Y.H.; Sun, B.J.; Xu, B.Y.; Chen, Y.; Zhao, X.X.; Chen, L.T. A Wellbore–Formation-Coupled Heat-Transfer Model in Deepwater Drilling and Its Application in the Prediction of Hydrate-Reservoir Dissociation. *J. SPE J.* **2017**, *22*, 756–766. [CrossRef]
14. Cheng, W.L.; Huang, Y.H.; Lu, D.T.; Yin, H.R. A novel analytical transient heat-conduction time function for heat transfer in steam injection wells considering the wellbore heat capacity. *J. Energy* **2011**, *36*, 4080–4088. [CrossRef]
15. Wang, Z.X.; Gao, D.; Fang, J. Numerical simulation of RF heating heavy oil reservoir based on the coupling between electromagnetic and temperature field. *J. Fuel* **2018**, *220*, 14–24. [CrossRef]
16. Li, M.Z.; Chen, H.J.; Zhang, Y.Y.; Li, W.W.; Wang, Y.P.; Yu, M. A Coupled Reservoir/Wellbore Model to Simulate the Steam Injection Performance of Horizontal Wells. *J. Energy Technol.* **2015**, *3*, 535–542. [CrossRef]
17. Xiao, D.; Hu, Y.F.; Meng, Y.F.; Li, G.; Wang, T.D.; Chen, W.X. Research on wellbore temperature control and heat extraction methods while drilling in high-temperature wells. *J. Pet. Sci. Eng.* **2022**, *209*, 109814. [CrossRef]
18. Mao, D.M.; Xie, X.X.; Jones, R.M.; Harvey, A.; Karanikas, J.M. A Simple Approach for Quantifying Accelerated Production Through Heating Producer Wells. *J. SPE J.* **2017**, *22*, 316–326. [CrossRef]
19. You, J.Y.; Rahnema, H.; McMillan, M.D. Numerical modeling of unsteady-state wellbore heat transmission. *J. Nat. Gas Sci. Eng.* **2016**, *34*, 1062–1076. [CrossRef]
20. Ge, S. *Transient Temperature and Pressure Coupling Model of Gas Well Borehole*; Southwest Petroleum University: Chengdu, China, 2015.
21. Zhong, H.Q.; Zheng, C.G.; Li, M.; Liu, T.; He, Y.F.; Li, Z.H. Transient Pressure and Temperature Analysis of a Deepwater Gas Well during a Blowout Test. *J. Process.* **2022**, *10*, 846. [CrossRef]
22. Lin, R.Y.; Wang, F.Z.; Wang, X.W. Heating of heavy oil by circulating hot water in closed double casing in ultra-deep wells. *J. Pet. Sci.* **2019**, *9*, 506–510. [CrossRef]
23. Nie, B. Circulating preheating model of full-length horizontal wellbore in heavy oil reservoirs with multiple thermal fluid injection. *J. Pet. Sci. Eng.* **2022**, *208*, 109215. [CrossRef]
24. Wan, N.H.; Wang, L.S.; Hou, L.T.; Wu, Q.L.; Xu, J.Y. Modeling Transient Flow in CO2 Injection Wells by Considering the Phase Change. *J. Process.* **2021**, *9*, 2164. [CrossRef]
25. Hasan, A.R.; Kabir, C.S. A Mechanistic Model for Computing Fluid Temperature Profiles in Gas-lift Wells. *J. SPE Prod. Oper.* **1996**, *11*, 179–185. [CrossRef]
26. Hasan, A.R.; Kabir, C.S.; Wang, X. A Robust Steady-state Model for Flowing-fluid Temperature in Complex Wells. *J. SPE Prod. Oper.* **2009**, *24*, 269–276. [CrossRef]
27. Hasan, A.R.; Kabir, C.S. Wellbore Heat-transfer Modeling and Applications. *J. Pet. Sci. Eng.* **2012**, *86*, 127–136. [CrossRef]